OPTOELECTRONIC CHARACTERISATION OF INTERMEDIATE BAND SOLAR CELLS BY PHOTOREFLECTANCE: COMPARISON TO OTHER ADVANCED ARCHITECTURES

Enrique Cánovas*, David Fuertes Marrón, Antonio Martí, Antonio Luque
Instituto de Energía Solar – ETSIT, Universidad Politécnica de Madrid, Ciudad Universitaria s.n., 28040 Madrid, Spain.
* Present address: FOM Institute AMOLF, Science Park 104, 1098 XG Amsterdam, The Netherlands.

Colin R. Stanley, Corrie D. Farmer
Department of Electronics and Electrical Engineering, University of Glasgow, Oakfield Av. G12 8LT Glasgow, U.K.

Andreas W. Bett
Fraunhofer-Institut für Solare Energiesysteme, Heidenhofstraße 2, 79110 Freiburg, Germany.

ABSTRACT: The fabrication and design of novel materials and devices for advanced photovoltaics, like the intermediate-band solar cell (IBSC), requires the use of specific characterization tools providing information about their optoelectronic properties. We have tested the suitability of photoreflectance for the characterization of IBSC prototypes based on quantum dots and compared the results obtained with those predicted by the theory. Nonidealities in operative devices have been identified and detailed information has been obtained about the electronic structure of the materials. We have compared PR spectra of IBSCs with those obtained from alternative device architectures, namely a triple-junction solar cell and a multi-quantum well structure. Some general conclusions are drawn demonstrating the potential of the technique.
Keywords: Intermediate band solar cell; photoreflectance.

1 INTRODUCTION

The intermediate band solar cell (IBSC) is a photovoltaic device with potential to surpass the theoretical efficiency limits of conventional solar cells [1]. The study of such devices has attracted attention from both theoreticians and experimentalists. As a result of such efforts, potential material candidates have been identified, key operational principles have been demonstrated and progress toward its practical implementation in working devices is ongoing [2].

The main feature of an IBSC is the utilization of a so-called intermediate band material (IBM) acting as light absorber. IBMs are characterized by a narrow intermediate band (IB) in the forbidden gap which is partially filled with charge carriers. The IB effectively divides the main gap of the absorber into two lower sub-bandgaps. The IBM presents thus three absorption onsets corresponding to electronic transitions from the valence band to the intermediate band and from the intermediate band to the conduction band, in addition to the conventional valence-to-conduction transition. The increased photocurrent stemming from sub-bandgap absorption as compared to the photocurrent expected from conventional valence-to-conduction transitions can lead to an increased photovoltaic conversion efficiency of a solar cell based on an IBM provided the output voltage is limited by the main gap of the absorber.

The complex electronic structure of IBMs requires characterisation tools able to test the quality of the material at an early stage, i.e., prior to device completion and metallization, particularly in designs operative under concentrated light. The *ideal* IBM characterisation method would be fast, contactless and sensitive to the main optoelectronic properties of IBMs, not requiring cryogenic cooling or vacuum/inert atmosphere during operation. Photoluminescence (PL) has been identified as a good candidate [3], though it normally requires high vacuum assisted by cooling units. Photoreflectance (PR) combines all advantages mentioned for the *ideal* characterization tool, appearing as robust complementary technique to PL and usually providing a wider range of information not easily accessible by other means. In this contribution we will comment briefly on the technique, present the expected features of PR spectra when applied to an ideal IBM, discuss the results obtained to date from the characterization of state-of-the-art IBMs, and finally compare such results to those obtained from alternative novel device architectures, namely multi-quantum well (MQW) absorbers and triple-junction solar cells.

2 EXPERIMENTAL BASICS

PR belongs to the group of electro-modulation techniques, which are in turn a variety of modulation spectroscopies. As such, it is basically an analogue method for taking the derivative of the optical spectrum of a material by modifying in some manner the measurement conditions [4]. The upper panel of Figure 1 represents the reflectance (R) spectrum of a typical semiconducting sample as a function of the photon energy. The step in R coincides with the occurrence of a critical point in the electronic structure of the sample (associated with inter-band or inter-sub-band resonances; *i.e.*, a bandgap). The transmittance (T) would show a similar behaviour but with the curve flipped around the energy of the bandgap. The step in T is typically larger than in R at the transparency threshold of the sample, but T is nominally zero for $E>E_g$ if the sample has a high absorptance. On the other hand, R is typically finite on both sides of the transparency threshold, except for especial cases (e.g., AR-coatings). The lower panels of Figure 1 represent derivatives of first up to the third order of R with respect to the energy. It can be observed that the derivative spectra somehow isolate the critical point out of R, neglecting minor changes of R away from the region of interest. The finite magnitude of R throughout the entire energy range avoids eventual indetermination of the derivative spectra, which could affect an analogue

analysis based on T. Furthermore, the sharpness of the signature in the third derivative spectrum is increased with respect to that of the first-derivative spectrum.

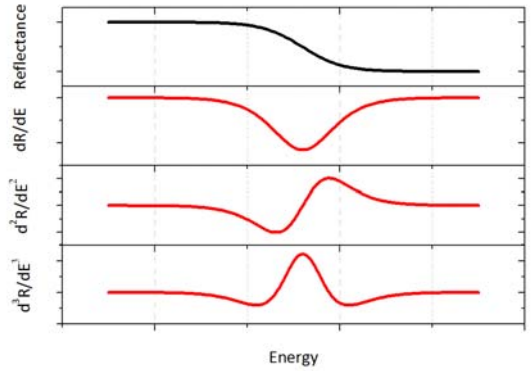

Figure 1: Reflectance spectrum (upper panel) and corresponding 1st, 2nd and 3rd derivative spectra with respect to the energy (lower panels) of a typical semiconducting sample.

Electro-modulation uses an electric field as a perturbing agent. In particular, PR relies on the diffusion of optically generated charge carriers (without the need for electrical contacts) to modulate electric fields associated with space-charge regions, typically present at surfaces and interfaces. The dielectric constants of the sample, and thereof its reflectance and transmittance, are thus perturbed upon application of a periodic modulation on the electric field. The presence of electric fields breaks the translational symmetry of electrons in the crystal lattice and can accelerate free carriers. It can be shown that this fact implies that the corresponding electro-modulated spectra will show a third-derivative line-shape at critical points associated to unbound electronic states [5]. However, bound states associated to excitons, impurities or uncoupled quantized levels at nanostructures do not possess translational symmetry and are confined in space. In such cases, the line-shape of electro-modulated spectra is first-derivative-like. We can therefore obtain information about the nature of the critical points observed in PR spectra by analyzing the line-shapes of the signatures. Notwithstanding, distinguishing first- and third-derivative line-shapes at first sight is usually not straightforward and numerical analysis are required. The general form of a third-derivative line-shape in an electro-modulated spectrum in the low field regime is given by the third-derivative functional form (TDFF) [5]:

$$\frac{\Delta R}{R} \propto (\hbar\Theta)^3 \times \mathrm{Re}\left\{ A e^{i\varphi} \left(E - E_g + i\Gamma \right)^{-m} \right\}, \qquad (1)$$

where A is the amplitude of the signal, Γ is a broadening factor, φ is a phase factor, E_g is the energy of the critical point, m depends on the type of critical point, and $\hbar\Theta$ is the electro-optic energy given by:

$$(\hbar\Theta)^3 = \frac{q^2 \hbar^2 F^2}{2\mu}, \qquad (2)$$

where F is the electric field and μ is the reduced inter-band effective mass in the direction of the field. The phase factor has a large impact on the appearance of the PR signal. Figure 2 shows the same TDFF, following Eq. 1, for three different phase factors (given in radians). Comparing these results with Figure 1, it follows that drawing conclusions about the third-derivative nature of a line-shape is not evident at first sight.

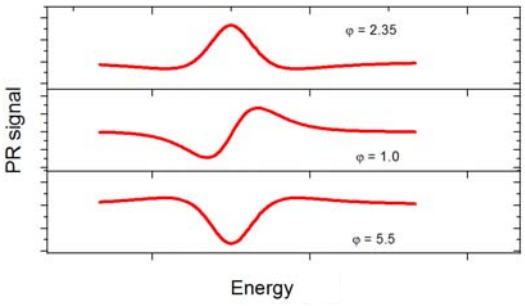

Figure 2: Simulated third-derivative line-shapes of a PR signal for different values of the phase factor, with all other parameters fixed.

The low-field regime in electo-modulated measurements is defined by $|\hbar\Theta| \leq \Gamma$. In the high-field case, $|\hbar\Theta| \geq \Gamma$ with $qFa_0 << E_g$, where a_0 is the lattice constant of the crystalline sample. This condition ensures that the band structure and the energies of the critical points are preserved. In the high-field regime, the dielectric function can exhibit Franz-Keldysh oscillations (FKO) [6]. This is reflected in a PR spectrum by an oscillatory behaviour of the signal at energies above that of the critical point associated, as it will be shown later. The origin of such behaviour is the tilting of the energy bands in the presence of the electric field (Stark effect). An electron attempting to tunnel from the valence into the conduction band will face a triangular energy barrier of width determined by the magnitude of the field. If during the tunneling process the electron interacts with a photon of energy $E>E_g$, the effective width of the barrier is reduced and the transmission probability includes an oscillatory term. The period of the oscillations is a direct measure of the magnitude of the electric field.

With PR we can therefore obtain detailed information about the existence of bandgaps and their nature (E_g and m-factor of TDFF); the Lorentzian broadening of the line-shapes (Γ); the bound or unbound character of the electronic states involved in transitions (derivative-order); and the electro-optic energy and the magnitude of associated electric fields at surfaces and interfaces, among other issues. It can be performed at ambient temperature, on wafer-sized material or locally at sub-millimeter scale, even *in-situ* during sample processing. It is non-destructive and typically does not require vacuum or an inert atmosphere. Furthermore, the diffusion of optically generated carriers allows buried interfaces far beyond the penetration depth of the optical pumping to be probed.

A typical experimental PR set-up is shown in Figure 3. The light beam of a tungsten lamp (250 W) is passed through a monochromator (1/8 m Cornerstone-Newport) and focused by optical lenses (not shown) on the surface of the sample. The light directly reflected is focused with lenses and measured with a solid-state detector (Si or Ge). The current signal is pre-amplified and transformed to a voltage (Keithley) and feeds the lock-in amplifier (Stanford Instruments). Superimposed onto the light spot at the surface of the sample, a laser beam (325 nm line of a 10 mW He-Cd laser) chopped mechanically at a certain

frequency (typically 777 Hz) provides the modulated perturbation. The energy of the pump laser beam determines the highest critical point accessible. The signal recorded at the detector contains two components: the dc average signal $I_0(\lambda)R(\lambda)$ and the ac modulated signal $I_0(\lambda)\Delta R(\lambda)$, where $\Delta R(\lambda)$ is the change in reflectance caused by the modulated perturbation. The lock-in tracks the ac signal at the given frequency. The relative change in reflectance is then obtained by normalizing the ac signal with respect to the dc component, giving typical values between 10^{-3} and 10^{-6}. Such normalization represents an additional advantage of the technique in terms of eventual incomplete light collection: provided enough light reaches the detector, the line-shape of the modulated spectrum is not affected by the loss of some light in I_0.

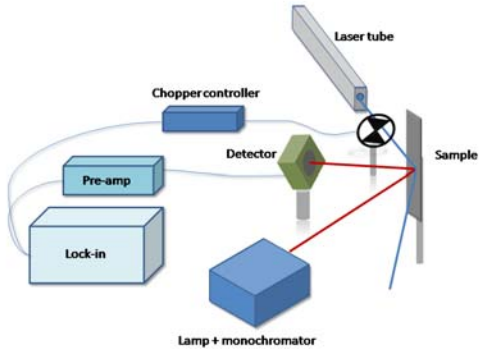

Figure 3: Schematic arrangement of PR setup.

2 PR ON IB-ARCHITECTURES

We turn now our attention to the application of PR to IBMs. The main optoelectronic feature of IBMs is the occurrence of three absorption onsets, corresponding to the three electronic transitions allowed. In the ideal case of an IBSC designed to operate under maximum sunlight concentration, such transitions occur at 1.93 eV (VB to CB), 1.23 eV and 0.7 eV (for those involving the IB). Figure 4 represents the calculated PR spectrum from the TDFF (Equ. 1) of such an IBM. The color code is only a guide to the eye denoting the energy range of each transition. For the calculation, identical broadening factors, phases and amplitudes have been considered in all three transitions for clarity. *m*-factors of 2.5, characteristic of 3-D critical points like the fundamental gap of GaAs, have been used. We have assumed that the critical points correspond to direct transitions, as desired for efficient light absorption. It should be mentioned that indirect transitions are PR-silent, although they can be probed by first-derivative techniques, like piezo-reflectance and thermo-reflectance, in which the modulated perturbation (strain or temperature gradients, respectively) are not associated with breaking of translational symmetry, like in the case of the electric field [7]. A PR spectrum similar to Figure 4 is expected for triple-junction solar cells, as discussed later.

Up to date, experimental attempts to fabricate IBMs can be classified into two categories: (i) those based on quantum-dot structures (QD-IBSC) and (ii) those based on alloys (bulk IBMs). PR has been successfully applied to a particular type of highly mismatched alloys characterized by the so-called band anti-crossing effect [8]. The electronic structure of such alloys is determined by the formation of a narrow band of electronic states isolated from the main band edges functioning as an IB. PR has indeed been used to demonstrate the band-anti-crossing mechanism governing the electronic structure.

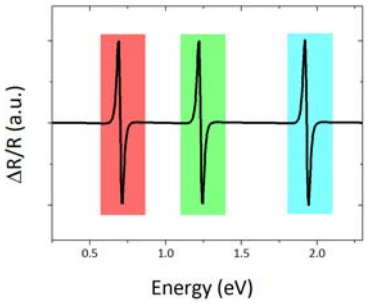

Figure 4: Calculated PR spectrum of an ideal IBM.

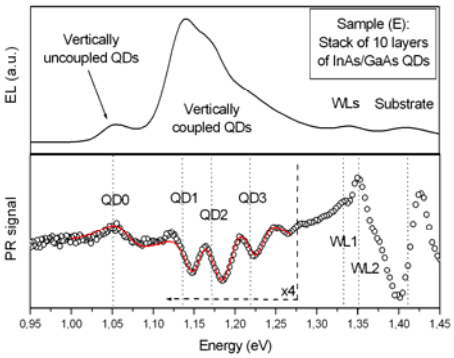

Figure 5: Experimental PR spectrum of a QD-IBSC prototype based on InAs/GaAs QDs (lower panel) and corresponding electro-luminescence (upper panel). The solid line is the fitted PR spectrum in the energy range controlled by the confined states [9].

PR has also been applied to QD-IBSC prototypes. Figure 5 [from Ref. 9] shows a PR spectrum of a device structure containing 10 layers of self-assembled InAs QDs embedded into GaAs. The analysis following the TDFF (Equ. 1) reveals several critical points associated with the ground and excited states of the QDs, as well as vertical coupling (unbound states) between them. Comparing Figures 4 and 5, it is evident that the QD-IBSC based on InAs/GaAs is far from the optimum structure. All transitions associated to the dots (QD) and the corresponding wetting layers (WL) would represent the experimental analog to the green single transition of Figure 4. The PR signature at 1.42 eV in Figure 5 corresponds to the bandgap of the barrier material and would, therefore, be the analogue of the blue transition of Figure 4. There is not only a significant shift of the experimental transitions with respect to optimal values, but also a number of optically active sub-bandgap transitions, also observed in the electro-luminescence spectrum of the same structure (Fig. 5 upper). The abundance of available levels, comparable to multiple intermediate bands, closely spaced between the green and blue domains of the ideal structure results in an effective shorting of the IB with the conduction band, with detrimental effects on the performance of the device, particularly on the output voltage. The InAs/GaAs QD-

IBSC has nevertheless proved very useful to test the key operational principles of the IBSC [10]. PR studies on both highly mismatched alloys and QD-IBSC have revealed two out of three transitions theoretically expected (those at high energies). Up to now, there is no experimental evidence from PR for the lowest energy transition in Fig. 4. The reason is the non-ideal position of the IB within the main bandgap in current prototypes that shifts the lowest energy transition to the mid infrared, thus only accessible with IR-detectors provided with cooling units. In addition, the optical transition in this energy range has to compete with thermal escape at room temperature. Current efforts are focused on this issue as such optical transition as part of the two-photon absorption process is a key marker of an IBSC.

3 COMPARISON TO OTHER ADVANCED DEVICE ARCHITECTURES

PR has also been used to study different advanced solar cell designs. Two examples are shown in Figure 6. The upper panel shows the PR spectrum of a metamorphic $Ge/Ga_{0.83}In_{0.17}As/Ga_{0.35}In_{0.65}P$ triple-junction solar cell with AlInP window [11]. Similar structures have demonstrated efficiency figures of 41.1% [12]. Figure 6 includes the schematic spectral decomposition corresponding to four absorption onsets (three absorbers plus window). The PR spectrum is dominated by FKOs above the fundamental gaps of $Ga_{0.83}In_{0.17}As$ and $Ga_{0.35}In_{0.65}P$ (absorption onsets of the middle and top cells). Multi-junction solar cells comprise a number of heterojunctions which develop space charge regions at the interfaces between layers of the stack. The presence of FKOs, together with the signatures stemming from critical points of the absorbers, does therefore characterize the PR spectra of multi-junction structures. The fact that the fundamental gap of Ge is PR-silent (indirect) prevents the observation of the lowest absorption onset. Further details, including the estimation of the fields, are presented elsewhere [11].

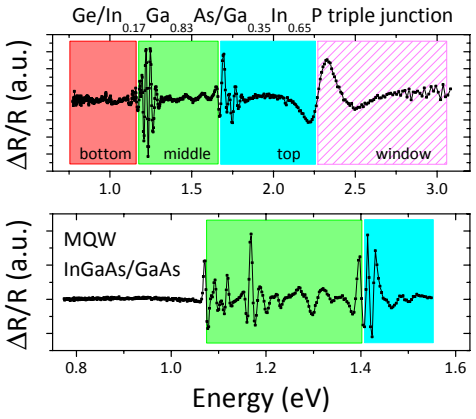

Figure 6: PR spectra of a $Ge/Ga_{0.83}In_{0.17}As/Ga_{0.35}In_{0.65}P$ triple-junction solar cell (uopper) and a MQW $In_{0.32}Ga_{0.68}As/GaAs$ structure (lower).

The lower panel of Figure 6 shows the PR spectrum of a multiple quantum well (MQW) structure consisting of 4 $In_{0.32}Ga_{0.68}As$ wells of varying thickness separated by GaAs barriers. Although the MQW structure resembles that of the QD-IBSC based on similar compounds, it should be stressed that the MQW solar cell is fundamentally limited in efficiency to figures comparable to those obtainable from a single solar cell made out of the same material as used for the wells. The reason of such limitation is the 2D-character of the electronic structure, which presents confinement only in the direction perpendicular to the plane of the layer. This fact implies a non-zero density of states between the discrete energy levels of the wells and the conduction band of the barrier material, with no effective separation of respective quasi-Fermi levels in operation (shorting). This leads in turn to output voltages limited by the hole- and electron-states in the wells and not by the barrier material, as required for IB-operation. In addition, selection rules in the electric dipole approximation normally inhibit optical absorption leading to inter-band transitions in the wells, at least in normal incidence [13]. As a result, optical pumping from confined states up into states resonant with the conduction band of the barrier material is not operative and the extraction of current from confined states relies entirely on thermal escape. For this reason, the schematic spectral distribution in Figure 6 does not include the third region at low energies (that would correspond to electrons optically pumped from confined states to conduction band) but rather ends up at the lowest transition associated with electrons pumped from hole-states up to confined states, slightly above 1 eV. As can be seen in the figure, the energy range associated with transitions involving states at the wells presents a number of critical points that extend to the vicinity of the fundamental gap of the barrier material. Its analysis will be presented elsewhere.

4 CONCLUSIONS

PR appears as an interesting tool for the characterization of IBSCs and it may serve as a diagnostic technique to assess the opto-electronic quality of IB-materials at an early stage of processing, as well as for other advanced device architectures.

Financial support from the EC (IBPOWER-211640), the Spanish Ministry of Science and Innovation (GENESIS FV-CSD2006-00004), and the Madrid Regional Council (NUMANCIA II-S05050/ENE/000310) is acknowledged.

REFERENCES

[1] A. Luque, A. Martí, Phys. Rev. Lett. 78 (1997) 5014.
[2] A. Luque, A. Martí, Adv. Mater. 22 (2010) 160.
[3] N. Ekins-Daukes *et al.* Proc. 31st IEEE PVSC (2005) 40.
[4] F.H. Pollak, Surf. Interface Anal. 31 (2001) 938.
[5] D.E. Aspnes, Surf. Sci. 37 (1973) 418.
[6] H. Shen, M. Dutta, J. Appl. Phys. 78 (1995) 2151.
[7] M. Cardona, *Modulation spectroscopy*, Academic Press (1969).
[8] W. Shan *et al.* Phys. Rev. Lett. 82 (1999) 1221.
[9] E. Cánovas *et al.* Proc. 23rd EPVSEC (2008) 298.
[10] A. Martí *et al.* Phys. Rev. Lett. 97 (2006) 247701.
[11] E. Cánovas, D. Fuertes Marrón, A. Martí, A. Luque, A.W. Bett, submitted to Appl. Phys. Lett.
[12] W. Guter *et al.* Appl. Phys. Lett. 94 (2009) 223504.
[13] J.P.Loher, M.O. Manasreh, *Semiconductor quantum wells and superlattices for IR-detectors,* Artech, 1993